Engineered symbiotic bacteria interfering *Nosema* redox system inhibit microsporidia parasitism in honeybees

Haoyu Lang[a], Hao Wang[a], Haoqing Wang[a], Xianbing Xie[b], Xiaosong Hu[a], Xue Zhang[c], Hao Zheng[a,*]

[a]College of Food Science and Nutritional Engineering, China Agricultural University, 100083 Beijing, China

[b]Department of laboratory animal science, Nanchang University, 330006 Nanchang, China

[c]College of Plant Protection, China Agricultural University, 100083 Beijing, China

*Hao Zheng, Email: hao.zheng@cau.edu.cn

Keywords: *Apis mellifera*, *Nosema ceranae*, gut microbiota, RNAi, reactive oxygen species

Abstract

Nosema ceranae is an emergent microsporidia parasite of the European honey bee (*Apis mellifera*), which causes serious nosemosis implicated in honeybee colony losses worldwide. *N. ceranae* is an obligate intracellular eukaryotic parasite that mainly invades the midgut of honeybees. Recent studies find that bee gut microbiota is potentially involved in protecting against parasitism. Here, using laboratory-generated bees mono-associated with gut members, we find that *Snodgrassella alvi* inhibited microsporidia proliferation, potentially via the stimulation of host oxidant-mediated immune response. Accordingly, *N. ceranae* employs the thioredoxin and glutathione systems to defend against oxidative stress and maintain a balanced redox equilibrium, which is essential for the infection process. We knocked down the gene expression using nanoparticle-mediated RNA interference, which targets the γ-glutamyl-cysteine synthetase and thioredoxin reductase genes of microsporidia. It significantly reduces the spore load, confirming the importance of the antioxidant mechanism for the intracellular invasion of the *N. ceranae* parasite. Finally, we genetically modified the symbiotic *S. alvi* to deliver dsRNA corresponding to the genes involved in the redox system of the microsporidia. The engineered *S. alvi* induces RNA interference and represses parasite gene expression, thereby inhibits the parasitism by up to 99.8%. Specifically, *N. ceranae* was most suppressed by the recombinant strain corresponding to the glutathione synthetase or by a mixture of bacteria expressing variable dsRNA. Our findings extend our previous understanding

of the protection of gut symbionts against *N. ceranae* and provide a symbiont-mediated RNAi system for inhibiting microsporidia infection in honeybees.

Introduction

Honey bees (*Apis mellifera*) are pollinators with global economic value responsible for pollinating ecologically and agriculturally valuable crops. For the past decade, a phenomenon known as Colony Collapse Disorder has posed a global threat to honeybee health. Recent studies suggest several factors involved in colony decline, such as parasite and pathogen invasion, pesticide use, and environmental stressors. Honeybees are susceptible to a variety of pathogens and pests, including bacteria[1], fungi[2], viruses[3], *Varroa* destructors[4], and microsporidian parasites[5].

The microsporidia are obligate intracellular eukaryotic parasites of honeybees and infect the midgut epithelial cells. Honeybees are mainly infected by two species of microsporidia that cause nosemosis, one of the most severe bee diseases worldwide[6]. *Nosema apis* was initially described in European honeybees and was considered the exclusive parasite species causing nosemosis. Later, another species *Nosema ceranae* was discovered in the Asian honeybee, *Apis cerana*, which is presumed to be the original host, and it may transfer to *A. mellifera* during the past decades[7]. It appears that *N. ceranae* displaces *N. apis* in *A. mellifera*, and the prevalence studies found that *N. apis* infections are becoming rarer than *N. ceranae*[8]. *N. ceranae* transmit via the fecal-oral route and the ingestion of spores from the contaminated hive materials[9]. It can suppress the immune defense mechanism of

43 honeybees, ensuring the infection of epithelial cells[10, 11]. The parasitic infection
44 reduces the lifespan and colony populations of *A. mellifera* and affects host
45 physiology and behaviors[12, 13].

46 Honeybees rely on innate immunity to defend against infectious agents, which
47 operate through cellular and humoral mechanisms[14]. The humoral immune system
48 consists of antimicrobial peptide production, which provides defense primarily against
49 bacterial pathogens. For intracellular parasites, insects can clear invading parasites by
50 eliciting oxidative stress[15, 16, 17]. The intestinal epithelial and macrophage cells
51 produce reactive oxygen species (ROS)[18], including superoxide anion (O_2^-), hydrogen
52 peroxide (H_2O_2), and hydroxyl radical (HO•). While there is no evidence that ROS is
53 effective in clearing microsporidia, the infection of *N. ceranae* may disrupt the
54 oxidative balance of the honeybee gut[19].

55 Host ROS production can be modulated by the gut microbiota to eliminate
56 opportunistic pathogens[18]. Although it is unclear whether the microbiota inhibits the
57 parasitism, *N. ceranae* infection perturbs the native gut composition, which may
58 enhance the intensity of the parasitic microsporidia[20]. The honeybee gut microbiota
59 typically contains five core bacterial members[21]. It has been shown that the bee gut
60 bacteria influence bee health by modulating host immune responses. Specifically,
61 *Snodgrassella alvi* and *Lactobacillus apis* protect honeybees from opportunistic
62 bacterial pathogens by inducing host immune response and AMPs production[22, 23].
63 Furthermore, the native gut bacteria can be engineered to better improve honeybee

health[24]. Leonard *et al*. recently genetically modified *S. alvi*, refining a system to induce RNAi within hosts. By expressing dsRNA to interfere gene expression of *Varroa* mite and DWV, the genetically engineered strains repress DWV and *Varroa* infection[25]. This symbiont-mediated RNAi provides a promising strategy for improving bee resistance against stressors.

Here, we investigate the effect of honeybee gut members on the inhibition of *N. ceranae* invasion. Specifically, *S. alvi* upregulated the expression of host genes related to the ROS-associated immune response and significantly repressed the proliferation of *N. ceranae*. Then, we evaluated the role of the antioxidant system of *N. ceranae* in the adaptation and reproduction in the midgut epithelia. We found that *N. ceranae* mainly employed the thioredoxin and glutathione systems to relieve the intense oxidative stress from the host for parasitism. Finally, we constructed recombinant *S. alvi* to continuously produce dsRNA corresponding to the thioredoxin and glutathione system-related genes of *N. ceranae*, significantly inhibiting the *N. ceranae* proliferation in the midgut cells.

Results

Gut bacteria aid in the clearance of the pathogenic *N. ceranae*

We first determined whether the core gut members prevent the invasion of *N. ceranae in vivo*. Gnotobiotic bees mono-associated with different gut bacteria, *Bifidobacterium choladohabitans* W8113, *Bombilactobacillus mellis* W8089,

84 *Lactobacillus apis* W8172*, Gilliamella apicola* B14384H2, and *Snodrgrassella alvi*
85 M0351, were generated in the lab. Microbiota-free honeybees were fed with pure
86 cultures of bacterial strains. After allowing the colonization of symbiotic strains in the
87 gut for seven days, each bee individual was manually infected with *N. ceranae* cell
88 suspensions of 10^4 spores by oral feeding (Fig. 1A). On Day 17, we quantified the
89 absolute abundance of *N. ceranae* spores in the midguts. It showed that the spore load
90 was significantly lowered in bees mono-colonized with *S. alvi*, while bees colonized
91 by other gut members did not show a significant reduction of *N. ceranae* (Fig. 1B).
92 Insects can clear parasites from invasion by eliciting oxidative stress,
93 primarily by producing ROS in gut epithelia[26, 27]. Thus, we assessed whether *S. alvi*
94 stimulated the production of ROS in the gut, which may fight against invading
95 intracellular *N. ceranae* parasite. In the honeybee, the production of ROS is mainly
96 regulated by the Nox/Duox NADPH oxidases, as in other insects[28]. We found that the
97 expression of genes encoding Duox and Nox were upregulated in the midgut of bees
98 24 h post-colonization by *S. alvi* M0351 (Fig. 1C, D). Correspondingly, both the
99 intracellular ROS signal tested by the fluorogenic sensor and the production of
100 hydrogen peroxide (H_2O_2) increased in the midgut following the colonization by *S.*
101 *alvi* (Fig. 2E, F). These results indicate that the colonization of the core gut member,
102 *S. alvi*, triggered the redox response involved in gut immunity, which may inhibit the
103 *N. ceranae* infection in the honeybees.

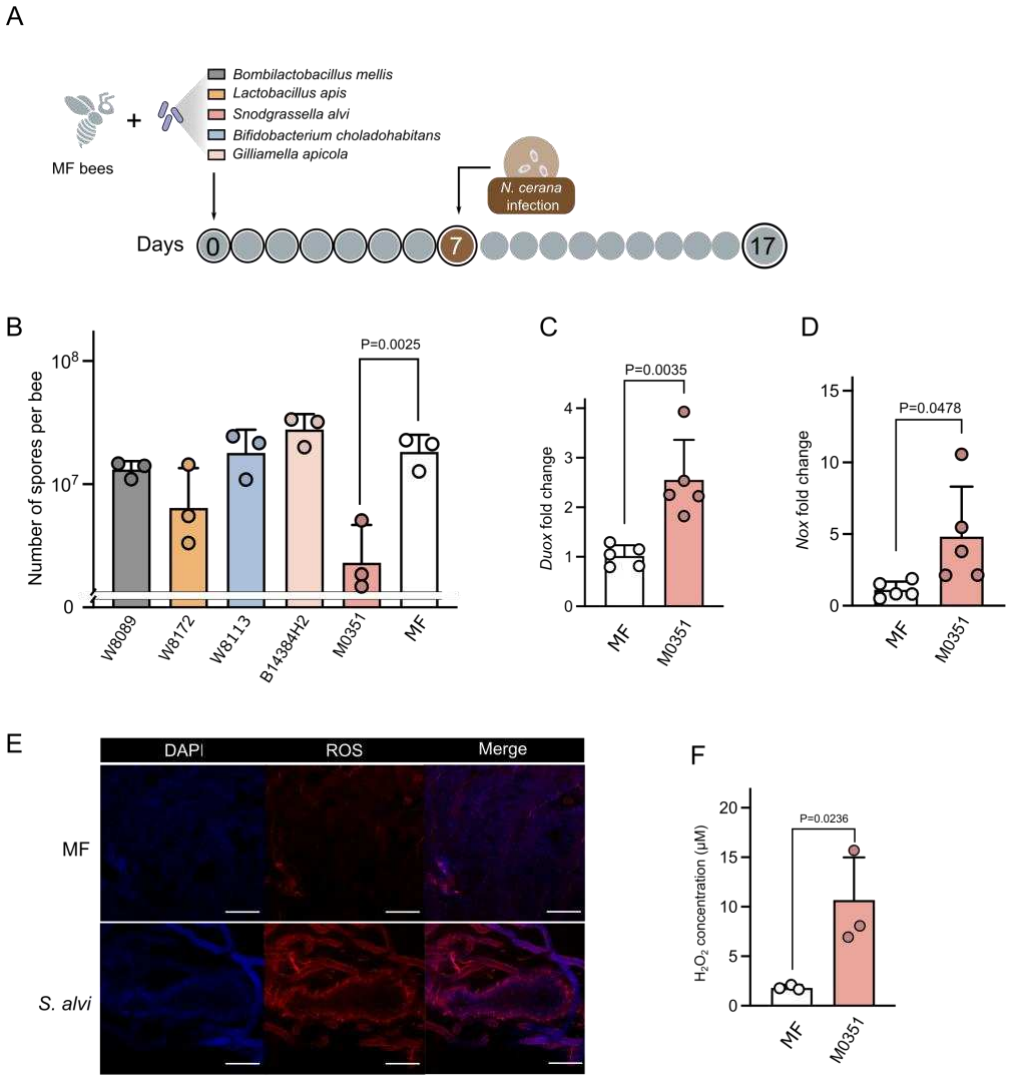

Fig. 1. *Snodgrassella* strains protect against *N. ceranae* via the ROS-associated immune response in the honeybee gut. (A) Schematic illustration of experimental design. Microbiota-free (MF) bees were colonized with *B. choladohabitans* W8113, *B. mellis* W8089, *L. apis* W8172, *G. apicola* B14384H2, and *S. alvi* M0351 for seven days and then orally infected with *N. ceranae*. (B) Absolute abundance of *N. ceranae* spores in the midgut 10 days post-infection with *N. ceranae*. (C-D) The expression level of the *Duox* and *Nox* genes in the midgut following *S. alvi* M0351 colonization. (E)

Fluorescence staining for ROS signal within the midgut cells of MF and mono-colonized bees with *S. alvi*. (F) H_2O_2 concentration in the midgut of MF and mono-colonized bees with *S. alvi*. Scale bars = 250 μm. Statistical analysis was performed by using multiple two-tailed t-test.

N. ceranae employs antioxidant systems to adapt and reproduce in the midgut epithelium

We have shown that ROS produced by the bees is implicated in the defense against *N. ceranae*, and typically, the parasites employ endogenous antioxidant systems to relieve intense oxidative stress[29, 30]. To examine the pathways used by *N. ceranae* to resist honeybee gut oxidative stress during infection, we reanalyzed an RNA-seq dataset that documents the changes in gene expression of *N. ceranae* when colonizing the bee gut[31]. *De novo* synthesis of reduced glutathione synthesized by γ-glutamyl-cysteine synthetase (γGCS) and glutathione synthetase (GS) is crucial in the antioxidant defense of *N. ceranae* (Fig. 2A). By following the time-series gene expression profiles, we found that both the expression of γGCS and GS of *N. ceranae* increased along with the infection (Fig. 2B, C). Moreover, glutathione can be further catalyzed by the Glutathione peroxidases (GPx) to reduce H_2O_2[32]. We identified that *N. ceranae* possessed two genes encoding GPx in the genome of *N. ceranae*, GPx-1(AAJ76_3500027152) and GPx-2 (AAJ76_3500027978). Interestingly, the

132 expression of GPx-1 increased during the first 3 days of infection, but GPx-2 was
133 downregulated during invasion (Fig. 2D, E). In addition, *N. ceranae* also possesses a
134 complete thioredoxin system, consisting of the key enzymes of thioredoxin reductase
135 (TrxR, AAJ76_5800012528) and thioredoxin peroxidase (TPx, AAJ76_280004776),
136 in defense against oxidative stress (Fig. 2F). We found that the expression of TrxR
137 and TPx genes of *N. ceranae* were elevated from day 2 post-infection (Fig. 2G, H).
138 To further validate the importance of the thioredoxin and glutathione redox
139 systems for the *N. ceranae* invasion, we knocked down γGCS from the glutathione
140 system and TrxR from the thioredoxin system, respectively. Here, we used the
141 nanoparticle-mediated dsRNA delivery system to improve RNAi efficiency[33]. By
142 feeding the nanoparticle-mediated dsRNA, the mRNA transcript levels of *N. ceranae*
143 γGCS and TrxR genes were reduced by ~80% on Day 10 and Day 15 after
144 inoculation. Microscopic observation confirmed that the proliferation of *N. ceranae*
145 was significantly depressed by both dsγGCS and dsTrxR silencing in the midgut.
146 Altogether, these results indicate that *N. ceranae* probably maintains the redox state
147 by employing the thioredoxin and glutathione systems to relieve the oxidative stress
148 from the host and to adapt and reproduce in the midgut epithelium[34]. This also implies
149 that host ROS-associated immunity is responsible for the defense against intracellular
150 parasitism in honeybees.

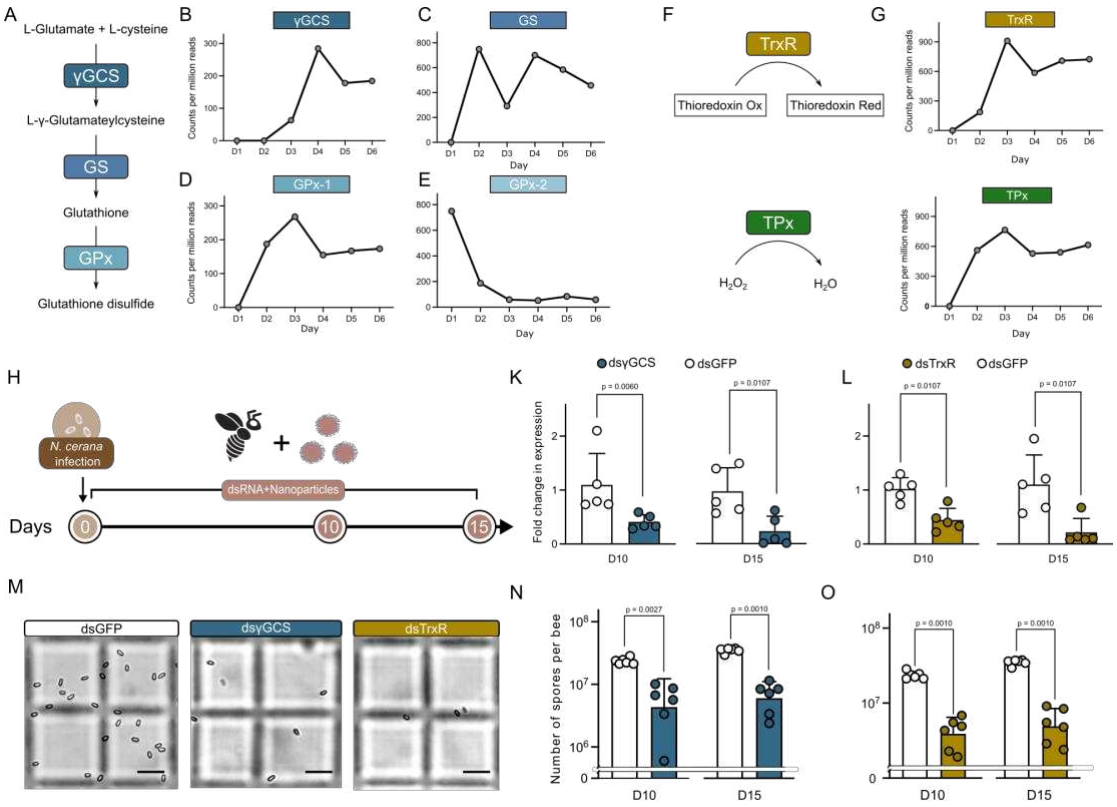

151

152 **Fig. 2.** The thioredoxin and glutathione systems of *N. ceranae* are significant

153 for the proliferation in the epithelial cells. (A) The glutathione system forms

154 glutathione by γ-glutamyl-cysteine and glutathione synthetases in *N. ceranae*.

155 (B-E) The expression level of the γGCS, GS, GPx-1, and GPx-2 genes over

156 the infection process. (F) *N. ceranae* possesses a complete thioredoxin

157 system consisting of the thioredoxin reductase and thioredoxin peroxidase.

158 (G) The expression level of the TrxR and TPx genes over the infection

159 process. (H) Knockdown of *N. ceranae* γGCS and TrxR gene expression by

160 feeding nanoparticle-mediated dsRNA. (K-L) Relative expressions of the

161 γGCS and TrxR genes of *N. ceranae* before and after RNAi on Days 10 and

162 15. (M) The load of *N. ceranae* spores was quantified by microscopy using a

163 hemocytometer. (N-O) Silencing of γGCS and TrxR genes inhibited *Nosema*

infection levels. Scale bars = 0.025mm. Statistical analysis was performed by the Mann-Whitney U test.

Inhibition of *N. ceranae* infection by engineered *S. alvi*

Since the antioxidant defense is crucial for *N. ceranae* parasitism, we next engineered *S. alvi* strain M0351 to produce dsRNA targeting microsporidian genes. First, we transformed strain M0351 with a stable plasmid pBTK519 expressing GFP from the Bee Microbiome Toolkit platform [24] and tested whether it could re-colonize bee gut robustly. The engineered strain M0351 was inoculated into newly emerged bees treated with ampicillin to eliminate native microbiota (Fig. 3A)[25]. We inoculated bee individuals with ~10^5 CFU of GFP-tagged *S. alvi*. They grew to ~8.0×10^7 CFU/bee after five days of colonization and persisted stably throughout the 15-day experiments (Fig. 3B). The majority of engineered *S. alvi* cells (~80%) remained functional with a high density of fluorescent signal, while some bacterial cells lost the fluorescence in the guts at the endpoint (Day 15; Fig. 3C). While *Snodgrassella* preferentially colonizes the ileum, they also distribute in all compartments of the bee gut[35]. The confocal microscopy showed that 15 days after colonization, the engineered M0351 effectively colonized both the ileum and midguts of 10 inspected bees, showing the same spatial distributions as the wild-type strain (Fig. 3D-F) [36]. Thus, our results showed that the engineered *S. alvi* could persistently colonize the

183 honeybee ileum and midgut, and the plasmid pBTK519 functioned reliably in strain

184 M0351 throughout the experiments.

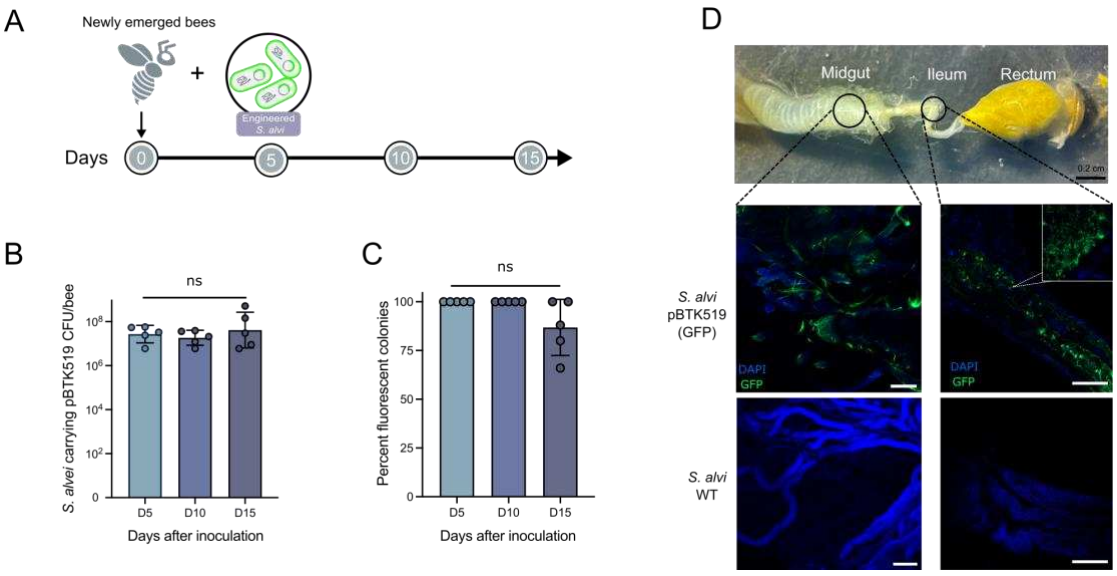

185

186 **Fig. 3.** The engineered *S. alvi* M0351 showed stable colonization and function

187 in bee guts. (A) Newly emerged bees were colonized with *S. alvi* transformed

188 with a plasmid expressing a green fluorescent protein. The colonization level

189 was checked on Days 5, 10, and 15. (B-C) Engineered *S. alvi* M0351 stably

190 colonized and expressed GFP continuously over time. Each dot represents an

191 individual bee sample. (D) Engineered *S. alvi* M0351 colonized both the

192 midgut and ileum of bees. Scale bars = 200 μm. Statistical analysis was

193 performed by the Mann-Whitney U test.

We have shown that *S. alvi*-treated honeybees prevent *N. ceranae* infection by triggering ROS production (Fig. 1), and *N. ceranae* employed the thioredoxin and glutathione system to relieve the intense oxidative stress (Fig. 2). Thus, we engineered *S. alvi* M0351 using plasmid pBTK519 to express dsRNA targeting the glutathione and thioredoxin systems of *N. ceranae*. Target sequences from the γGCS, GS, GPx-1, GPx-2, TrxR, and TPx genes were designed and amplified from the cDNA of *N. ceranae* (Fig. 4A; Fig. S1). Using the Bee Microbiome Toolkit, we assembled plasmids with an inverted arrangement of two promoters (pBTK150, pBTK151) and other previously designed parts for the production of dsRNA[24, 37]. We built six complete dsRNA-producing plasmids targeting different genes and transformed these plasmids into *S. alvi* M0351 by conjugation. We inoculated newly emerged honeybees with ~10^5 cells of *S. alvi* bearing different plasmids that expressed dsRNA corresponding to the GFP coding sequence (pDS-GFP) or those expressed target sequences. Then, the bees were challenged by oral feeding with *N. ceranae* spores (10^4 spores/bee), and 10 days later, we tested whether the *Snodgrassella*-produced dsRNA could inhibit the proliferation of *N. ceranae*.

We first extracted the RNA of *N. cerana* to confirm the depression of targeted pathways. Compared to the pDS-GFP off-target control, a significantly lower expression of target genes from *N. cerana* was identified (Fig 4B–G). Expression of all targeted genes is decreased by 50–86% in *N. ceranae* with different recombinant strains, suggesting that the dsRNA is delivered from the engineered *S. alvi* to allow

215 diffusion to the parasite. After 10 days of dsRNA silencing, we evaluated the
216 inhibitory capacity of various engineered *S. alvi* strains by quantifying the spore load
217 with microscopic observation. First, both the wild-type *S. alvi* and the pDS-GFP
218 provided protection compared with the controls without symbiont inoculation (Fig.
219 4H), confirming the role of *S. alvi* in defending against *N. ceranae*. Engineered *S. alvi*
220 strains expressing γGCS, GPx-1, GPx-2, TrxR, or TPx dsRNA had a 99%, 96%,
221 96.5%, 97.9%, and 98.2% decrease in *N. ceranae* spore load, respectively. Notably,
222 pDS-GS targeting the glutathione synthetase of the glutathione system showed the
223 highest inhibition (99.7%) of the microsporidia spore invasion. Moreover, we also
224 evaluated the effect of mixing engineered strains, and the inhibitory effect by a
225 mixture of bacteria delivering all six dsRNA was better than the colonization with
226 single strains.

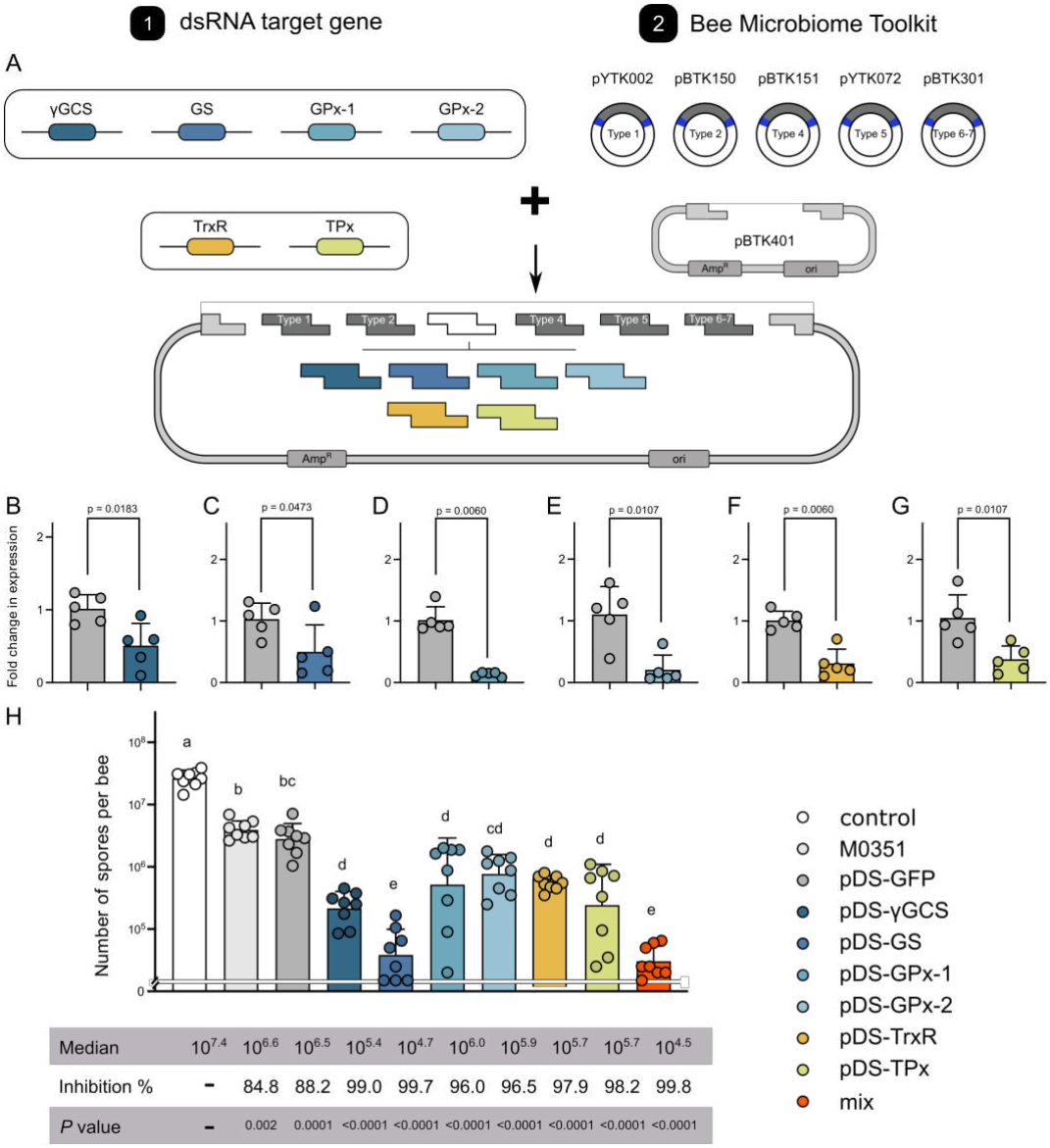

Median	$10^{7.4}$	$10^{6.6}$	$10^{6.5}$	$10^{5.4}$	$10^{4.7}$	$10^{6.0}$	$10^{5.9}$	$10^{5.7}$	$10^{5.7}$	$10^{4.5}$
Inhibition %	-	84.8	88.2	99.0	99.7	96.0	96.5	97.9	98.2	99.8
P value	-	0.002	0.0001	<0.0001	<0.0001	<0.0001	<0.0001	<0.0001	<0.0001	<0.0001

Fig. 4. Recombinant *S. alvi* M0351 strains engineered to deliver dsRNA inhibit the infection of *N. ceranae*. (A) Schematic illustration of the Golden Gate assembly strategy for constructing plasmids expressing targeted dsRNA. (B-G) Engineered *S. alvi* strains to produce dsRNA targeting genes of the thioredoxin and glutathione systems inhibited the gene expression of *N. ceranae* in the midgut. (H) Inhibition of *N. ceranae* infection by engineered *S. alvi* M0351 strains. Each dot represents the spores number of an individual

bee in the midgut. Letters above each bar stand for statistical differences between sampling sites (least-significant difference (LSD) test, $P < 0.05$). The median number of spores of each treatment group and the percent inhibition (inhibition %) of spore load relative to the non-colonized control are indicated.

Discussion

Nosema ceranae is a microsporidian parasite initially identified from the *Apis cerana* in the 1990s[38] and later detected in different honeybee species worldwide, becoming a globally distributed pathogen[27]. In this study, we found that *N. ceranae* employs the thioredoxin and glutathione system to relieve oxidative stress from the host for the adaptation in the midgut epithelium (Fig. 5). We showed that the core gut bacteria, *S. alvi*, triggers the redox response involved in honeybee gut immunity, which inhibits the proliferation of *N. ceranae* by up to 85.5%. Moreover, we successfully constructed engineered *S. alvi* M0351 based on the Bee Microbiome Toolkit and the Functional Genomics Using Engineered Symbionts procedure (FUGUES) to continuously produce dsRNA for critical genes of the *N. ceranae* thioredoxin and glutathione systems. Engineered *S. alvi* can stably re-colonize bees and repress the parasite's thioredoxin and glutathione system-related gene expression. The γGCS and GS of the glutathione system are the most effective targeted genes for *N. ceranae* inhibition. Furthermore, the inhibitory effect by the mixture of all six engineered *S. alvi* strains showed the highest inhibition (99.8%).

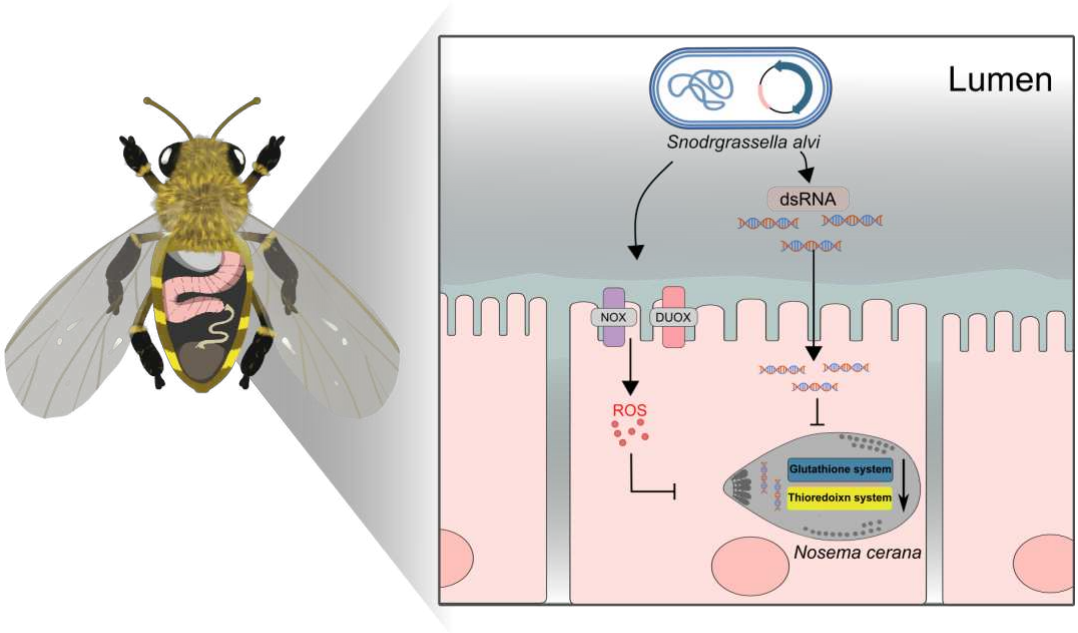

Fig. 5. Graphical summary of the *N. ceranae* inhibition by the engineered *S. alvi* M0351 strains. By triggering *Duox* and *Nox* genes, *S. alvi* induces ROS production in the midgut of honeybees, which may kill *N. ceranae* via perturbation of redox homeostasis. *N. ceranae* may employ the thioredoxin and glutathione antioxidant systems to relieve the intense oxidative stress for intracellular proliferation. Engineered *S. alvi* M0351 expressing the dsRNA corresponding to the genes of the oxidation-reduction systems of *N. ceranae* can significantly inhibit parasitism in the honeybee gut.

The microsporidia *N. ceranae* is an obligate intracellular parasite that develops in the ventricular epithelia of *A. mellifera*, and the spores can spread the infection quickly across epithelial cells[39]. The concept that the immune activation of honey

bees plays a role against *N. ceranae* is not new, but the exact mechanism remains unclear. In all invertebrates, including insects, the adaptive system is missing, and hence, defense is entirely ensured by the innate immune system. The innate immune system provides organisms with a rapid, non-specific first line of defense against colonization by pathogenic microorganisms[40]. Honeybees' cell-mediated innate immune system consists of hemocytes, which produce ROS essential for cell signaling and pathogen clearance[41]. ROS are produced during the recognition and phagocytosis response against the foreign bodies inside the cells[42]. In insects, ROS was shown to be particularly important in the fight against parasites and pathogenic bacteria in the gut[27, 43]. The production of ROS has been observed following the infection of *Aedes aegypti* mosquito by different microsporidian species[44]. In honeybees, genes involved in the production of ROS are overrepresented in the midgut upon the spore infection, suggesting that the increased ROS level is an immune response against intracellular parasitism[19]. Our results confirmed that the ROS-associated immune response in the epithelial cells is indispensable for preventing microsporidia infection in bees.

Two ROS-producing enzymes, the NADPH oxidases Duox and Nox, are identified in *A. mellifera*, similar to *Drosophila*. Here, we found that the expression of both *Duox* and *Nox* genes was activated in the midgut of bees post-colonization by *S. alvi*. It has been documented that *S. alvi* protects honeybees from the opportunistic pathogen *Serratia marcescens* by triggering the Toll and Imd pathway to upregulate

the expression of host antimicrobial peptides abaecin, apidaecin, and hymenoptaecin[45]. *S. alvi* colonizes the honeybee gut in contact with the gut epithelia and forms a dense biofilm, which may stimulate pattern recognition receptors such as Toll-like receptors of bees[45]. Interestingly, the activation of Toll-like receptors possibly conjugates the NADPH oxidases, which are involved in the ROS production on the membranes of the endosome of cells[46]. Notably, bees mono-colonized with *S. alvi* strain inhibit the proliferation of *N. ceranae* by up to 85.5%. In contrast, bees colonized by other gut members did not show a significant reduction of *N. cerana.* Thus, the ROS immune response may be activated by *S. alvi* by regulating the Toll signaling and the NADPH complex. The ROS system is also a gut-immune immune response involved in gut-microbe homeostasis[18]. In honeybees, the *N. ceranae* infection can perturb the gut composition, and a normal microbiota is required for host resistance to *N. ceranae*[47, 48]. The bore gut members of honeybees, including the *S. alvi* and *Lactobacillus apis*, have been shown to activate the humoral innate immune system to produce antimicrobial peptide (AMP), which protects against pathogens[22, 23]. Our data shows that the bee gut bacteria also plays a pivotal role in controlling microsporidia invasion by inducing de novo generation of ROS[18].

To protect itself against host defenses of ROS, the parasite may have an internal antioxidant system to maintain a normal redox state. For example, *Plasmodium falciparum* scavenges ROS from hosts by employing antioxidant systems, including the NADPH-dependent thioredoxin and the glutathione system [34,

309 [49]. We found that *N. ceranae* also possesses balanced redox pathways, including the
310 thioredoxin and glutathione systems, which may be necessary for counteracting ROS
311 attacks from the host. Analyzing the time series of gene expression of *N. ceranae*
312 colonizing the bee gut, we found significant upregulation in the expression of
313 thioredoxin and glutathione system genes, suggesting that the maintenance of the
314 normal redox state is significant in the invasion process of *N. ceranae*. Previous
315 studies that used RNAi targeting on variable *N. ceranae* genes, such as the polar tube
316 protein 3 (ptp3) and the spore wall protein (SWP), reduce parasite load and improve
317 the physiological performance of honeybees[50, 51]. Our results showed that the delivery
318 of dsRNA corresponding to γGCS and TrxR led to a significant reduction in spore
319 load by 82% and 85%, respectively, indicating that the endogenous antioxidant
320 enzymes of *N. ceranae* provide a novel therapeutic target for the control of the
321 parasitic invasion in honeybees.

322 Although RNAi is widely used, it is expensive for application in agricultural
323 fields, and its efficiency is also unsatisfactory. Recently, researchers have engineered
324 host-associated bacterium to produce dsRNA as a novel delivery modality. Taracena
325 *et al*. used engineered *Escherichia coli* to produce dsRNA to control the *Rhodnius*
326 *prolixus* parasite, a vector of the Chagas disease[52]. Although laboratory *E. coli* is easy
327 to be engineered, the symbiotic bacteria with minimal fitness cost and stable
328 association with the host are more promising for *in vivo* treatment [53]. Recently,
329 Leonard *et al*. have designed the Functional Genomics Using Engineered Symbionts

330 (FUGUES) procedure for engineering the native bacterial species of honeybees[25]. The
331 engineered *S. alvi* produces dsRNA to inhibit parasitic *Varroa* by inducing mite RNAi
332 response[37]. It documents that the RNA produced by the recombinant strains can be
333 transported to the gut, hemolymph, and head of bees, which alters host physiology
334 and behavior. *N. ceranae* infects and proliferates intracellularly in the epithelial cells
335 of the midgut[38]. While *Snodgrassella* mainly localizes to the ileum region of the
336 hindgut, it also colonizes the midgut intensively[35]. Our results illustrated that the
337 recombinant *S. alvi* strain stably re-colonizes both ileum and midgut post-inoculation,
338 and the plasmid exhibit a robust expression *in vivo*. Thus, the dsRNA produced by the
339 symbiotic *S. alvi* may enter into the midgut cells and destroy the redox homeostasis of
340 *N. ceranae*. Here, we targeted all six genes involved in the glutathione and
341 thioredoxin systems of the microsporidia. Interestingly, the repression of the GS gene
342 showed the highest inhibition efficiency. GS is not subject to feedback inhibition by
343 GSH and is important in determining overall GSH synthetic capacity, specifically
344 under pathological conditions[54]. In addition, the inhibition of a mixture of the
345 recombinant strains is more significant than the single-targeting strains, suggesting a
346 more effective perturbation of the parasitic antioxidant system. *S. alvi* and other bee
347 gut bacteria can be naturally transmitted within the colony via social contact, and
348 engineered *S. alvi* strains are transferred between co-housed bees, which suggests that
349 the use of native gut bacteria can facilitate the treatment of individual bees from an
350 entire colony[37]. Although gene escape is a major ethical issue for the application of

351 engineered bacteria, honeybee symbiotic bacteria are generally restricted to the bee
352 gut environment[21]. Moreover, *S. alvi* shows even more strict host specificity that only
353 specific strains are associated with different bee species or even individuals within the
354 colony[55]. Thus, symbiont-mediated RNAi provides a new tool to improve resilience
355 against current and future challenges to honey bee health.

356 # Materials and Methods

357 **Generation of microbiota-free and mono-colonized honeybees**

358 Honeybees (*A. mellifera*) used in this study were from colonies maintained in
359 the experimental apiary of the China Agricultural University. Pupae and newly
360 emerged bees used in all the experiments were obtained from brood frames taken
361 from the experimental hives and kept in an incubator at 35 °C, with a humidity of
362 50%. All honeybee gut bacterial strains used in this study are listed in Table S1.
363 *Snodgrassella alvi* M0351, *Bifidobacterium choladohabitans* W8113, and *Gilliamella*
364 *apicola* B14384H2 isolated from honeybee guts were grown on HIA supplemented
365 with 5% (vol/vol) sterile sheep blood (Solarbio). *Bombilactobacillus mellis* W8089
366 and *Lactobacillus apis* W8172 were grown on MRS agar plates (Solarbio)
367 supplemented with 0.1% L-cystine and 2.0% fructose.

368 Microbiota-free (MF) bees were obtained as described by Zheng *et al.*[56]. In
369 brief, we manually removed pupae from brood frames and placed them in sterile
370 plastic bins. Newly emerged MF bees were kept in axenic cup cages with sterile

371 sucrose syrup for 24h. For each mono-colonization setup, 20–25 MF bees were placed
372 in a cup cage and fed bacterial culture solutions for 24 hours. Colonization levels
373 were determined by colony-forming units from dissected guts, as described by Kwong
374 *et al*.[56] 1 mL of 1×PBS was combined with 1 mL of sucrose solution and 0.3 g of
375 sterilized pollen for the MF group. For the mono-colonization bees, glycerol stock of
376 bee gut strains was resuspended in 1 mL 1×PBS at a final concentration of ~10^8
377 CFU/mL and then mixed with 1 mL sterilized sucrose solution with 0.3 g of sterilized
378 pollen. The bees were incubated at 35°C and RH 50% until Day 7.

379 **_N. ceranae_ spore purification**

380 *N. ceranae* spores were isolated from worker honeybees collected from
381 heavily infected colonies in the summer of 2022. After immobilizing bees by chilling
382 them on ice, the guts were removed from individual bees with forceps. The midguts of
383 infected honeybees were homogenized in distilled water and filtered using Whatman
384 filtering paper. The filtered suspension was centrifuged at 3,000×g for 5 minutes, and
385 the supernatant was discarded. The re-suspended pellet was purified on a
386 discontinuous Percoll (Sigma-Aldrich, St. Louis, MO) gradient of 5 ml each of 25%,
387 50%, 75%, and 100% Percoll solution. The spore suspension was overlaid onto the
388 gradient and centrifuged at 8,000 × g for 10 minutes at 4°C. The supernatant was
389 discarded, and the spore pellet was washed by centrifugation and suspension in
390 distilled sterile water[57]. The number of spores was quantified using a Fuchs-Rosenthal
391 hemocytometer. The identity of the isolated *N. ceranae* or *N. apis* was determined by

392 amplifying the ribosomal RNA gene sequences with species-specific primers (Table
393 S3)[58].

394 **Bees mono-colonized with gut symbionts challenged with *N. ceranae***

395 To accurately control the number of *N. ceranae* cells infecting each bee
396 individual, bees were orally fed the same amount of *N. ceranae* spores. Each bee was
397 starved for 2 hours and given 2 µl of a 50% sucrose solution containing 10^4 *N.*
398 *ceranae* spores. After 10 days, the number of spores in the intestinal specimen of
399 infected bees was quantified as described by Huang *et al.*[47]. The midguts were
400 dissected, resuspended in 500 µl of double-distilled water, and then subjected to
401 vortex mixing. The suspension was put onto the hemocytometer for microscopic
402 observation.

403 **Honeybee gut RNA extraction and quantitative PCR**

404 Each dissected gut was homogenized with a plastic pestle, and total RNA was
405 extracted from individual samples using a Zymo Quick-RNA Tissue/Insect Microprep
406 Kit (Zymo Research, #R2030). RNA was eluted into 50 µL of RNase-free water and
407 stored at −80 °C prior to reverse transcription. cDNA was synthesized using the
408 HiScript III All-in-one RT SuperMix Perfect for qPCR (Vazyme). Quantitative real-
409 time PCR was performed using the ChamQ Universal SYBR qPCR Master Mix
410 (Vazyme) and QuantStudio 1 Real-Time PCR Instrument (Thermo Fisher Scientific,
411 Waltham, MA, USA) in a standard 96-well block (20-µl reactions; incubation at

95 °C for 3 min, 40 cycles of denaturation at 95 °C for 10 s, annealing/extension at 60 °C for 20 s). The primers for the genes of *Duox* (LOC551970) and *Nox* (LOC408451) of *A. mellifera* were designed with IDT qPCR PrimerQuest Tool (https://www.idtdna.com/pages/tools/primerquest) (Table S3). The actin gene of *A. mellifera* was used as the control, and the relative expression was calculated using the $2^{-\Delta\Delta CT}$ method [59].

In vivo detection of reactive oxygen species

Three days after inoculation, the midguts of the honeybees mono-colonized with *S. alvi* M0351 and the MF bees were dissected in PBS containing 50 μM intracellular ROS-sensitive fluorescent dye dihydroethidium (Invitrogen, #C10422). The tubes were placed in the dark for 10 min at room temperature. Then, the midguts were washed twice with a fresh dye-free PBS, and the tissues were immediately transferred to an μ-Dish$^{35\ mm,\ high}$ microscope dishes (Ibidi, #81156). We imaged the gut tissues on a Zeiss 910 Laser Scanning Confocal microscope with a 20× objective.

Measurement of the H_2O_2 production

The generation of H_2O_2 was determined using the Hydrogen Peroxide Assay Kit (Beyotime Biotech). In this assay, H_2O_2 converts Fe^{2+} to Fe^{3+}, which then reacts with xylenol orange dye to become purple with a maximum absorbance at 560 nm. The midguts were homogenized in 200 μL lysis buffer and centrifuged at 12,000 × g at 4 °C for 5 min, and the supernatant was collected. Aliquots of 50 μL of

supernatants and 100 μL of test solutions from the Hydrogen Peroxide Assay Kit were incubated at room temperature for 20 minutes and measured immediately with a spectrometer at a wavelength of 560 nm. The measurement was repeated three times for each sample.

RNA isolation of *N. ceranae*

To extract the RNA of *N. ceranae*, the honeybee gut was individually transferred into 2 ml tubes. Each tube contained 100 μL sterile 1.4-mm zirconium silicate grinding beads (Quackenbush). One milliliter of TRIzol reagent (Ambion) was added to the tube, disrupting the samples using the FastPrep. The samples were treated with DNase I (Invitrogen) to remove genomic DNA contamination. The purity and quantity of RNA samples were determined using a NanoDrop 8000 spectrophotometer (Thermo Fisher Scientific). cDNA was synthesized using the HiScript III All-in-one RT SuperMix Perfect for qPCR (Vazyme) and stored at –20°C.

***Nosema* inoculation and Nanocarrier-mediated dsRNA feeding assay**

To produce the double-stranded RNA of the γGCS (AAJ76_1100057370) and TrxR (AAJ76_5800012528) genes, the coding regions of the genes were amplified from *N. ceranae* cDNA with forward and reverse primers containing the T7 promoter sequence at their 5′ends (5′-TAATACGACTCACTATAGGGCGA-3′). The partially amplified segments of the genes were cloned into the pCE2-TA-Blunt-Zero vector

(Vazyme, China) and verified by Sanger sequencing. The fragment was amplified from the plasmid using specific primers with a T7 promoter and then used for dsRNA synthesis using the T7 RNAi Transcription Kit (Vazyme, China). The fragment amplified from the GFP gene (MH423581.1) was used as the control. The sequences of the primers are given in Table S3. Here, we used the star polycation as a gene nanocarrier to protect dsRNA molecules from enzymatic degradation and promote their translocation across cell membranes[60]. The nanocarrier was mixed with γGCS and TrxR dsRNA gently at a mass ratio of 1:1. (The final concentration for both SPc and dsRNA was 100 ng/μL.) The final concentrations for dsRNA + nanocarrier, and sucrose were 100 ng/μl and 50% (wt/vol), respectively. Newly emerged bees were removed from the frames and kept without food for at least 2 h before the subsequent *N. ceranae* inoculation. Individual bees were fed 2 μL of spores suspensions prepared by mixing purified spores into 50% sucrose (~10^4 spores/μL). From the day after *N. ceranae* inoculation, honeybees from each treatment were fed on different dsRNA mixtures in an incubator at 35°C The dsRNA mixture was supplied daily, and each bee ingested about 10 μg of dsRNA per day.

The treatment effect of dsRNA was determined by comparing the spore production rate for individual honey bees. The *N. ceranae* spore production rate was measured by counting the spores from the extracted midgut of live honey bees 15 days after inoculation. To investigate the effect of dsRNA treatment on the expression of each target gene of *Nosema*, qRT-PCR was performed after 15 days of dsRNA

473 treatment. After extracting the midguts from honeybees treated with *Nosema* and
474 dsRNA, the total RNA was extracted. cDNA was synthesized using the HiScript III
475 All-in-one RT SuperMix Perfect for qPCR (Vazyme). Each gene-specific primer is
476 given in Table S3. The β-tubulin gene of the *N. ceranae* was used as the control, and
477 relative expression was analyzed using the $2^{-\Delta\Delta CT}$ method [59].

478 **Vector construction to express dsRNA expression and *S. alvi* M0351**
479 **egineering**

480 All the plasmids and MFD*pir* were kindly donated by the Moran Lab and
481 Barrick Lab (University of Texas at Austin). We designed dsRNA-producing plasmid
482 parts based on the previously published Bee Microbiome Toolkit and functional
483 genomics using engineered symbionts procedure (FUGUES) (Fig. 4A)[25]. First, PCR is
484 used to amplify the knockdown region γGCS, GS, GPx-1, GPx-2, TrxR, and TPx
485 from the cDNA of *N. ceranae* and append BsaI cut sites to each end. Following PCR,
486 amplicons are purified and cloned into a dsRNA expression vector. We combined
487 previously designed parts pYTK002 (Type 1), pBTK150(Type 2), pBTK151(Type 4),
488 pYTK072 (Type 5), pBTK301 (Type 6-7), and pBTK401 (Type 8) (Addgene_65109,
489 Addgene_183127, Addgene_65179, Addgene_183126, Addgene_110593,
490 Addgene_110597), and dsRNA target sequence (Type 3) to assemble complete
491 plasmids that express dsRNA of the target sequence[37]. Golden Gate assembly
492 reactions were performed as previously described[24], and enzyme BsaI-HFv2 (New
493 England Biolabs) was used to increase assembly efficiency.

494 Assemblies were transformed into electroporated into *E. coli* donor strain
495 MFD*pir*. The plasmids were verified with Sanger sequencing. MFD*pir* cells with the
496 dsRNA expression vector and *S. alvi* cells are grown, washed, and combined to
497 initiate conjugation. Then, this mixture is plated on media containing 0.30 mM DAP.
498 The next day, cells are scraped, washed, and plated on media containing 100 µg/mL
499 ampicillin but without DAP to select for *S. alvi* cells that have acquired the plasmid
500 and against MFD*pir* cells. Transconjugant *S. alvi* colonies are passaged onto a second
501 plate containing 100 µg/mL ampicillin. These transconjugants can be confirmed to be
502 pure *S. alvi* cultures by performing 16S rRNA sequencing to ensure no unexpected
503 contaminants have been introduced during the conjugation process.
504 After 2–3 d of growth, we scraped the engineered *S. alvi* grown on the plates into
505 PBS. These cells were spun in a centrifuge (3824 × g, 5 min) and then resuspended in
506 500 µL PBS. Engineered *S. alvi* was diluted in 500 µL 1×PBS at a final concentration
507 of ~10^8 CFU/mL and combined with 500 µL of a 1:1 sucrose: water solution
508 supplemented with 200 µg/mL ampicillin. We fed engineered *S. alvi* solutions to age-
509 controlled newly emerged worker bees for 24 h (pDS-γGCS, pDS-GS, pDS-GPx-1,
510 pDS-GPx-2, pDS-TrxR, pDS-TPx) and non-targeted (pDS-GFP) served as a negative
511 control group. The next day, each bee was given 2 µl of a 50% sucrose solution
512 containing 10^4 *N. ceranae* spores. After ten days, honeybee gut was collected to
513 quantify the number of *N. ceranae* spores, and gene knockdown was validated using
514 qPCR on the cDNA of *N. ceranae* synthesized as described above.

To test whether engineered *S. alvi* robustly colonizes bees, we inoculated bees with *S. alvi* transformed with a plasmid expressing GFP. Firstly, we transformed strain M0351 with a stable plasmid pBTK519 expressing GFP from the Bee Microbiome Toolkit platform [24] and inoculated bees with *S. alvi* M0351::pBTK519 (~10^5cfu/bee). After every five days, we dissected bees, homogenized their whole guts in 500 µL PBS, and plated dilutions onto HIA plates with a final concentration of 100 µg/mL ampicillin to estimate CFUs of *S. alvi* in the gut. The number of fluorescent and non-fluorescent colonies on the plates was quantified to track the stability of engineered strains over time. After 15 days, we dissected the guts and imaged them on a Laser Scanning Confocal microscope.

Acknowledgments

We thank the Moran Lab and Barrick Lab (University of Texas at Austin) for donating plasmids. We thank Elijah Powell, Jeffrey Barrick, and Nancy Moran for their suggestions in gut bacteria engineering. We thank Jie Shen and Shuo Yan (China Agricultural University) for their assistance in the nanoparticle RNA delivery system. This work was supported by National Key R&D Program of China (Grant No. 2019YFA0906500), National Natural Science Foundation of China Project 32170495 and 31760715.

References

1. Funfhaus A, Ebeling J, Genersch E. Bacterial pathogens of bees. *Curr. Opin. Insect Sci.* **26**, 89-96 (2018).

2. Gerdts JR, Roberts JMK, Simone-Finstrom M, Ogbourne SM, Tucci J. Genetic variation of Ascosphaera apis and colony attributes do not explain chalkbrood disease outbreaks in Australian honey bees. *J. Invertebr. Pathol.* **180**, 107540 (2021).

3. Martin SJ, Brettell LE. Deformed Wing Virus in Honeybees and Other Insects. *Annu. Rev. Virol.* **6**, 49-69 (2019).

4. Traynor KS*, et al.* Varroa destructor: A Complex Parasite, Crippling Honey Bees Worldwide. *Trends Parasitol.* **36**, 592-606 (2020).

5. Burnham AJ. Scientific Advances in Controlling *Nosema ceranae* (Microsporidia) Infections in Honey Bees (Apis mellifera). *Front. Vet. Sci.* **6**, 79 (2019).

6. Fries I. *Nosema ceranae* in European honey bees (*Apis mellifera*). *J. Invertebr. Pathol.* **103 Suppl 1**, S73-79 (2010).

7. Martin-Hernandez R*, et al. Nosema ceranae* in Apis mellifera: a 12 years postdetection perspective. *Environ. Microbiol.* **20**, 1302-1329 (2018).

8. Milbrath MO*, et al.* Comparative virulence and competition between *Nosema apis* and *Nosema ceranae* in honey bees (*Apis mellifera*). *J. Invertebr. Pathol.* **125**, 9-15 (2015).

9. Chen Y, Evans JD, Smith IB, Pettis JS. *Nosema ceranae* is a long-present and wide-spread microsporidian infection of the European honey bee (*Apis mellifera*) in the United States. *J. Invertebr. Pathol.* **97**, 186-188 (2008).

10. Aufauvre J, Misme-Aucouturier B, Vigues B, Texier C, Delbac F, Blot N. Transcriptome analyses of the honeybee response to *Nosema ceranae* and insecticides. *PLoS ONE* **9**, e91686 (2014).

11. Antunez K, Martin-Hernandez R, Prieto L, Meana A, Zunino P, Higes M. Immune suppression in the honey bee (*Apis mellifera*) following infection by *Nosema ceranae* (Microsporidia). *Environ. Microbiol.* **11**, 2284-2290 (2009).

12. Paris L, El Alaoui H, Delbac F, Diogon M. Effects of the gut parasite *Nosema ceranae* on honey bee physiology and behavior. *Curr. Opin. Insect. Sci.* **26**, 149-154 (2018).

13. Gage SL, Kramer C, Calle S, Carroll M, Heien M, DeGrandi-Hoffman G. *Nosema ceranae* parasitism impacts olfactory learning and memory and neurochemistry in honey bees (Apis mellifera). *J. Exp. Biol.* **221**, (2018).

14. Evans JD*, et al.* Immune pathways and defence mechanisms in honey bees *Apis mellifera*. *Insect Mol. Biol.* **15**, 645-656 (2006).

15. Molina-Cruz A*, et al.* Reactive oxygen species modulate *Anopheles gambiae* immunity against bacteria and Plasmodium. *J. Biol. Chem.* **283**, 3217-3223 (2008).

16. Biron DG, Agnew P, Marche L, Renault L, Sidobre C, Michalakis Y. Proteome of Aedes aegypti larvae in response to infection by the intracellular parasite *Vavraia culicis*. *Int. J. Parasitol.* **35**, 1385-1397 (2005).

17. Panek J*, et al.* Hijacking of host cellular functions by an intracellular parasite, the microsporidian *Anncaliia algerae*. *PLoS ONE* **9**, e100791 (2014).

18. Ha EM, Oh CT, Bae YS, Lee WJ. A direct role for dual oxidase in *Drosophila* gut immunity. *Science* **310**, 847-850 (2005).

19. Dussaubat C*, et al.* Gut pathology and responses to the microsporidium Nosema ceranae in the honey bee *Apis mellifera*. *PLoS ONE* **7**, e37017 (2012).

20. Rubanov A, Russell KA, Rothman JA, Nieh JC, McFrederick QS. Intensity of *Nosema ceranae* infection is associated with specific honey bee gut bacteria and weakly associated with gut microbiome structure. *Sci. Rep.* **9**, 3820 (2019).

21. Kwong WK, Moran NA. Gut microbial communities of social bees. *Nat. Rev. Microbiol.* **14**, 374-384 (2016).

22. Lang H*, et al.* Specific Strains of Honeybee Gut *Lactobacillus* Stimulate Host Immune System to Protect against Pathogenic *Hafnia alvei*. *Microbiol. Spectr.* **10**, e0189621 (2022).

23. Kwong WK, Mancenido AL, Moran NA. Immune system stimulation by the native gut microbiota of honey bees. *R. Soc. Open. Sci.* **4**, 170003 (2017).

24. Leonard SP, *et al.* Genetic Engineering of Bee Gut Microbiome Bacteria with a Toolkit for Modular Assembly of Broad-Host-Range Plasmids. *ACS Synth. Biol.* **7**, 1279-1290 (2018).

25. Lariviere PJ, Leonard SP, Horak RD, Powell JE, Barrick JE. Honey bee functional genomics using symbiont-mediated RNAi. *Nat. Protoc.*, (2022).

26. Kumar S, *et al.* The role of reactive oxygen species on *Plasmodium* melanotic encapsulation in *Anopheles gambiae*. *Proc. Natl. Acad. Sci. U. S. A.* **100**, 14139-14144 (2003).

27. Diaz-Albiter H, Sant'Anna MR, Genta FA, Dillon RJ. Reactive oxygen species-mediated immunity against Leishmania mexicana and *Serratia marcescens* in the sand phlebotomine fly *Lutzomyia longipalpis*. *J. Biol. Chem.* **287**, 23995-24003 (2012).

28. Kawahara T, Quinn MT, Lambeth JD. Molecular evolution of the reactive oxygen-generating NADPH oxidase (Nox/Duox) family of enzymes. *BMC Evol. Biol.* **7**, 109 (2007).

29. Rahlfs S, Schirmer RH, Becker K. The thioredoxin system of Plasmodium falciparum and other parasites. *Cell Mol. Life. Sci.* **59**, 1024-1041 (2002).

30. Muller S. Role and Regulation of Glutathione Metabolism in Plasmodium falciparum. *Molecules* **20**, 10511-10534 (2015).

31. Huang Q, Chen YP, Wang RW, Cheng S, Evans JD. Host-Parasite Interactions and Purifying Selection in a Microsporidian Parasite of Honey Bees. *PLoS ONE* **11**, e0147549 (2016).

32. Brigelius-Flohe R, Flohe L. Regulatory Phenomena in the Glutathione Peroxidase Superfamily. *Antioxid. Redox. Signal.* **33**, 498-516 (2020).

33. Jin L, Wang Q, Chen J, Wang Z, Xin H, Zhang D. Efficient Delivery of Therapeutic siRNA by Fe(3)O(4) Magnetic Nanoparticles into Oral Cancer Cells. *Pharmaceutics* **11**, (2019).

34. Jortzik E, Becker K. Thioredoxin and glutathione systems in Plasmodium falciparum. *Int. J. Med. Microbiol.* **302**, 187-194 (2012).

35. Martinson VG, Moy J, Moran NA. Establishment of characteristic gut bacteria during development of the honeybee worker. *Appl. Environ. Microbiol.* **78**, 2830-2840 (2012).

36. Li Y, Leonard SP, Powell JE, Moran NA. Species divergence in gut-restricted bacteria of social bees. *Proc. Natl. Acad. Sci. U. S. A.* **119**, e2115013119 (2022).

37. Leonard SP*, et al.* Engineered symbionts activate honey bee immunity and limit pathogens. *Science* **367**, 573-576 (2020).

38. Fries I, Feng F, da Silva A, Slemenda SB, Pieniazek NJ. Nosema ceranae n. sp. (Microspora, Nosematidae), morphological and molecular characterization of a microsporidian parasite of the Asian honey bee Apis cerana (Hymenoptera, Apidae). *Eur. J. Protistol.* **32**, 356-365 (1996).

39. Higes M, Garcia-Palencia P, Martin-Hernandez R, Meana A. Experimental infection of Apis mellifera honeybees with Nosema ceranae (Microsporidia). *J Invertebr. Pathol.* **94**, 211-217 (2007).

40. Diamond G, Beckloff N, Weinberg A, Kisich KO. The roles of antimicrobial peptides in innate host defense. *Curr. Pharm. Des.* **15**, 2377-2392 (2009).

41. Richardson RT, Ballinger MN, Qian F, Christman JW, Johnson RM. Morphological and functional characterization of honey bee, Apis mellifera, hemocyte cell communities. *Apidologie* **49**, 397-410 (2018).

42. Kohchi C, Inagawa H, Nishizawa T, Soma G. ROS and innate immunity. *Anticancer. Res.* **29**, 817-821 (2009).

43. Buchon N, Silverman N, Cherry S. Immunity in Drosophila melanogaster--from microbial recognition to whole-organism physiology. *Nat. Rev. Immunol.* **14**, 796-810 (2014).

44. Duncan AB*, et al.* Proteome of Aedes aegypti in response to infection and coinfection with microsporidian parasites. *Ecol. Evol.* **2**, 681-694 (2012).

45. Horak RD, Leonard SP, Moran NA. Symbionts shape host innate immunity in honeybees. *Proc. Biol. Sci.* **287**, 20201184 (2020).

46. Park HS, Jung HY, Park EY, Kim J, Lee WJ, Bae YS. Cutting edge: direct interaction of TLR4 with NAD(P)H oxidase 4 isozyme is essential for

lipopolysaccharide-induced production of reactive oxygen species and activation of NF-kappa B. *J. Immunol.* **173**, 3589-3593 (2004).

47. Huang SK, *et al.* Influence of Feeding Type and Nosema ceranae Infection on the Gut Microbiota of Apis cerana Workers. *mSystems* **3**, (2018).

48. Li JH, *et al.* New evidence showing that the destruction of gut bacteria by antibiotic treatment could increase the honey bee's vulnerability to Nosema infection. *PLoS ONE* **12**, e0187505 (2017).

49. Bozdech Z, Ginsburg H. Antioxidant defense in Plasmodium falciparum--data mining of the transcriptome. *Malar. J.* **3**, 23 (2004).

50. Rodriguez-Garcia C, *et al.* Nosemosis control in European honey bees, *Apis mellifera*, by silencing the gene encoding *Nosema ceranae* polar tube protein 3. *J. Exp. Biol.* **221**, (2018).

51. Ma Z, Wang Y, Huang Z, Cheng S, Xu J, Zhou Z. Isolation of protein-free chitin spore coats of Nosema ceranae and its application to screen the interactive spore wall proteins. *Arch. Microbiol.* **203**, 2727-2733 (2021).

52. Taracena ML, *et al.* Genetically modifying the insect gut microbiota to control Chagas disease vectors through systemic RNAi. *PLoS Negl. Trop. Dis.* **9**, e0003358 (2015).

53. Wang S, *et al.* Driving mosquito refractoriness to Plasmodium falciparum with engineered symbiotic bacteria. *Science* **357**, 1399-1402 (2017).

54. Lu SC. Regulation of glutathione synthesis. *Mol. Aspects. Med.* **30**, 42-59 (2009).

55. Wu J, *et al.* Honey bee genetics shape the strain-level structure of gut microbiota in social transmission. *Microbiome* **9**, 225 (2021).

56. Zheng H, *et al.* Division of labor in honey bee gut microbiota for plant polysaccharide digestion. *Proc. Natl. Acad. Sci. U. S. A.* **116**, 25909-25916 (2019).

57. Cornman RS, *et al.* Genomic analyses of the microsporidian Nosema ceranae, an emergent pathogen of honey bees. *PLoS Pathog.* **5**, e1000466 (2009).

740 58. Schwarz RS, Evans JD. Single and mixed-species trypanosome and
741 microsporidia infections elicit distinct, ephemeral cellular and humoral
742 immune responses in honey bees. *Dev. Comp. Immunol.* **40**, 300-310 (2013).
743
744 59. Livak KJ, Schmittgen TD. Analysis of relative gene expression data using
745 real-time quantitative PCR and the 2(-Delta Delta C(T)) Method. *Methods* **25**,
746 402-408 (2001).
747
748 60. Zhang L*, et al.* Nanodelivery System Alters an Insect Growth Regulator's
749 Action Mode: From Oral Feeding to Topical Application. *ACS Appl. Mater.*
750 *Interfaces.* **14**, 35105-35113 (2022).
751
752 61. He N*, et al.* RNA Interference-Mediated Knockdown of Genes Encoding
753 Spore Wall Proteins Confers Protection against *Nosema ceranae* Infection in
754 the European Honey Bee, Apis mellifera. *Microorganisms* **9**, (2021).
755
756 62. Azzouz-Olden F, Hunt A, DeGrandi-Hoffman G. Transcriptional response of
757 honey bee (Apis mellifera) to differential nutritional status and *Nosema*
758 infection. *BMC Genomics* **19**, 628 (2018).
759
760

Supplementary Information

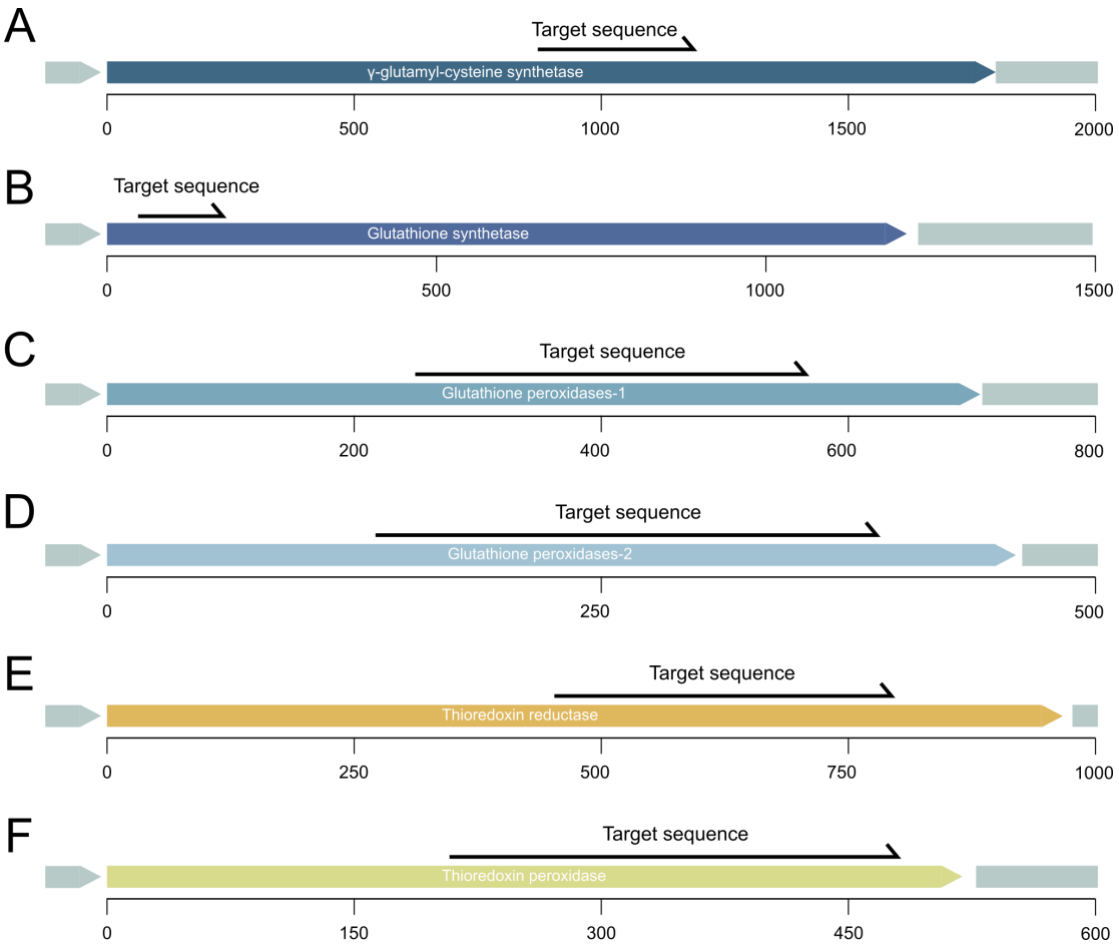

Fig. S1. Design of *N. ceranae* targets. This diagram shows the overall gene organization for *N. ceranae* γ-glutamyl-cysteine synthetase (A), glutathione synthetase (B), Glutathione peroxidases-1 (C), Glutathione peroxidases-2 (D), thioredoxin reductase (E), and thioredoxin peroxidase (F). The targeted region in each gene is denoted, and the designed target sequences are listed in Table S4.

769

770 **Table S1**. List of bacterial strains.

771

Species and strain	Source
E. coli MFD*pir*	[24]
E. coli DH5α	Vazyme
Snodgrassella alvi M0351	This study
Bifidobacterium choladohabitans W8113	This study
Bombilactobacillus mellis W8089	This study
Lactobacillus apis W8172	This study
Gilliamella apicola B14384H2	This study
Snodgrassella alvi M0351	This study

772

773 **Table S2**. Plasmid list.

774

Name	Use	Source
pBTK519	Constitutive GFP	[24]
pYTK002	Type 2 YTK/BTK connector sequence part plasmid	[24]
pYTK072	Type 5 YTK/BTK connector sequence part plasmid	[24]
pBTK301	Type 6-7 BTK bridge connector sequence part plasmid	[24]
pBTK401	Type 8 origin of replication and origin of transfer plasmid, *rsf1010* broad-host-range origin	[24]
pBTK150	Type 2 BTK part: terminator, CP25 promoter, no RBS	[37]
pBTK151	Type 4 BTK part: reverse CP25 promoter, terminator, no RBS	[37]
pYTK001_T1T2	Insulated part vector with flanking terminators	[37]
pDS-GFP	Control dsRNA GFP	[37]
pDS-γGCS	dsRNA target γGCS	This Study
pDS-GS	dsRNA target GS	This Study
pDS-GPx-1	dsRNA target GPx-1	This Study
pDS-GPx-2	dsRNA target GPx-2	This Study
pDS-TrxR	dsRNA target TrxR	This Study
pDS-TPx	dsRNA target TPx	This Study

775

Table S3. Primer list.

Purpose	Gene	Source	Forward	Reverse
qPCR	β-tubulin(*N. ceranae*)	[61]	AGAACCAGGAACGATGGAGA	TCCTTGCAAACAATCTGCAC
qPCR	Duox (*A.mellifera*)	[62]	CCCTAATAGCCCTCGTGAAC 3	GAGCATTCTCATAACGTGTG
qPCR	Nox (*A.mellifera*)	This study	ACCTGCTCTGTTTGGTCTCG	ACATCCACCACGTCGAACAA
qPCR	Glutamate-cysteine ligase catalytic subunit(*N. ceranae*)	This study	AACAGGCGAGGGAAGAAACC	CAACCCATACCTTGGCCCAT
qPCR	Glutathione synthetase (*N. ceranae*)	This study	TGGGAGTTTAATCGTTCTTGATGG	TCTAAACCGCCATTGCCAGA
qPCR	Glutathione peroxidase (*N. ceranae*)	This study	GGCAAATCCACATGTAGAAGC	TCTGCTATAGACTACAAAGACAAGA
qPCR	Glutathione peroxidase (*N. ceranae*)	This study	TGCAGTTGATTCAAAACAGTCAC	AGGCCTTTGTCATAAAATTCGTCT
qPCR	Thioredoxin reductase (*N. ceranae*)	This study	GTGGTCCTGCAGCCTATTCT	TACTTCCTACCATCCCGCCT
qPCR	Thioredoxin peroxidase (*N. ceranae*)	This study	TGATTTTACTTTTGTGTGTCCAACT	CACCGTCCTGTCTTGGGAG
RNAI_Type3	Glutamate-cysteine ligase catalytic subunit (*N. ceranae*)	This study	cGGTCTCatatgCCAAAAAGCAGGTGTTCTCCA	tGGTCTCaggatGGGAGTTGCTTGCATTTCCAT
RNAI_Type3	Glutathione synthetase (*N. ceranae*)	This study	cGGTCTCatatgGCTAGAGCGGTGGGTTTAGT	tGGTCTCaggatACCAAATGATACAAAACACTGTGAA
RNAI_Type3	Glutathione peroxidase (*N. ceranae*)	This study	cGGTCTCatatgGCGCACTTCTAGACGATCTCC	tGGTCTCaggatACATGTGGATTTGCCAAGAGT
RNAI_Type3	Glutathione peroxidase (*N. ceranae*)	This study	cGGTCTCatatgTTCCTTGTTCGCAATTTTTAAACCA	tGGTCTCaggatATAACCTCTGTTGGTCCATATCGC
RNAI_Type3	Thioredoxin reductase (*N. ceranae*)	This study	cGGTCTCatatgAGGAGGAGACTCTGCTATGGA	tGGTCTCaggatCGCAGTCGTACAATCCTCGT
RNAI_Type3	Thioredoxin peroxidase (*N. ceranae*)	This study	cGGTCTCatatgACGTTGTCAGTGATAGGAAGGA	tGGTCTCaggatACACATGATCCATTGCGTCCA
ds_RNAi	Glutamate-cysteine ligase catalytic subunit (*N. ceranae*)	This study	TAATACGACTCACTATAGGGTTGGATTTCTGGGCAACGGT	TAATACGACTCACTATAGGGCGAACCTCGTCAGCAAAAGG
ds_RNAi	Thioredoxin reductase (*N. ceranae*)	This study	TAATACGACTCACTATAGGGAGGAGGAGACTCTGCTATGGA	TAATACGACTCACTATAGGGCGCAGTCGTACAATCCTCGT
N. apis	rRNA (*N. apis*)	[58]	CCATTGCCGGATAAGAGAGT	TATATTTATTGTATTGCGCGTGCT
N. ceranae	rRNA (*N. ceranae*)	[58]	AGAAACTACAACAGCATCACTGGGA	AGTGAATATTCCAATTCCCAACGACTT

Table S4. Target sequences of dsRNA.

ID	Use	Length (bp)	GC %	Sequence Source
pDS-γGCS	γGCS knockdown	339	35	This Study
CCAAAAAGCAGGTGTTCTCCATTTGATTTATTTATTTCTAATGACGCTAGAAATTTAGACAAGTACAACGATACAAATCCACCG ATCCACGTGCCGATTTTTAATAAATTAATAAAGAAAGGTGTTGATGAAAAATTGTCGCGACATGTAGCATCTTTATTTATTCGC GATCCTATAGTCTCATATGACGAAACAGATGAAAGCACATTTGACGATTTTGAAAACATACAAAGTTCAAATTGGAGATCTGTA AGGTTTAAAGTACCAACAGAAAGTTCTGATAAAGATTTAAGAGGATGGAAAGTTGAAGTTCGTCCTATGGAAATGCAAGCAAC TCCC				
pDS-GS	GS knockdown	330	27	This Study
GCTAGAGCGGTGGGTTTAGTAAATCCATCTACAGGAAACATACTAAATATAACTATAAGACCCTCTAAAATATCAAGATTACAT TTTTTATCGATAAAAAATTTACAATTAAAACTTAATTTACTGTACTACAATCTAAGCAAAGACTTAGATTCATACACTTTTGATGA ACCAATGTACAAATTTTTGCACTCGATTTACACTGAAAAAAAAATGGTAAAAAAAGACAATATAGTAGCACTTTATATTAGATCT GATTATTTATTAGACGGTGACCAATATAAACAAGTAGAAATTAATACTATTTCACAGTGTTTTGTATCATTTGGT				
pDS-GPx-1	GPx-1 knockdown	348	28	This Study
ACATGTGGATTTGCCAAGAGTAATCTTTCTATACTAGCTGATATTATGACACTGTATAAAGAATATGGCCTTAAAATATTGATC TTTCCTTGTCTGCAATATTCAAAAGATGATACTGATTTACTTAAAAAGATGTATAACTTAATAACAGAATATTCTGATGATTTTA CAGTATTTAGTGATATTAATTTGGTCGGTAAAAATATACATCCTGTTTATAAGCATATTGTAAGGTATAGAAAAGAGTTTGTAG GAGATTTTATAAAATGGAATTTCGCAAAATTTATTGTTAATGAATACGGTGAAATAGTAAAAATTTTTGAACCAGGAGATCGTC TAGAAGTGCGC				
pDS-GPx-2	GPx-2 knockdown	250	30	This Study
TTCCTTGTTCGCAATTTTTAAACCAGGAATCTGGTGATATTGAAACTATTCGCAATTATGCGCATTCTATTTCTGATAAATTTAT CGTATTTGACAAAGTTAATGTATTTGGATCTCAAAAAGATCCTGTTTTTAAGTATTTAACAGACAACAGTTCAGAAAGTTTTTTT AAGTTTGTAAAATGGAACTTTACAAAATGGGTTGTTAAAGATGGAAAGATTTTAAAGCGATATGGACCAACAGAGGTTAT				
pDS-TrxR	TrxR knockdown	349	28	This Study
AGGAGGAGACTCTGCTATGGAAGAAGTCTTATTTTTATCTAAAATATGTTCTAAAGTTTATTTAATTCATCGAAGAAATGAATTT AGAAGCAGGAAGGATAAATTAGAAGAAGTAAAGAAGACAAAAAATATAGTTATAGTTACACCATATAATCTAAAATCTGCCCAT GGAATTGATAAATTAGAATATATTATCCTTGAAAATGGGGCAGAAACTAAAAAATTAGAAGTAGATGGATTGTTCTTTGGTATC GGTCATACACCTAATACTCAATTTTTAGAAGAAAATTTTTTACATGTTTTAGACAAAGATAAGTTTATTAAAGTAAACGAGGATT GTACGACTGCG				
pDS-TPx	TPx knockdown	330	37	This Study
ACGTTGTCAGTGATAGGAAGGAAGAGTTTATTAAACGCAATGTTGTTGTGTTTACAATTTCTAAAGATTCCGCATACAATCATC AAGCATGGGCTAAACTCCCAAGACAGGACGGTGGCGTAGAAGGAATACAATGGCCAATGTTGGCAGATAAGAATGCTCGTT TAAGTCGACAGTTTGGTTTGTATGATGATGAGGAAGATATCACCAAAAGGGCTACTGTAATGATTGATGTTTCTGGAAATGTG TTTAATATTTCTATCTATCATGAAAAAATAGGAAGAAATGTTGATGAAATTTTGAGGTTATTGGACGCAATGGATCATGTGT				